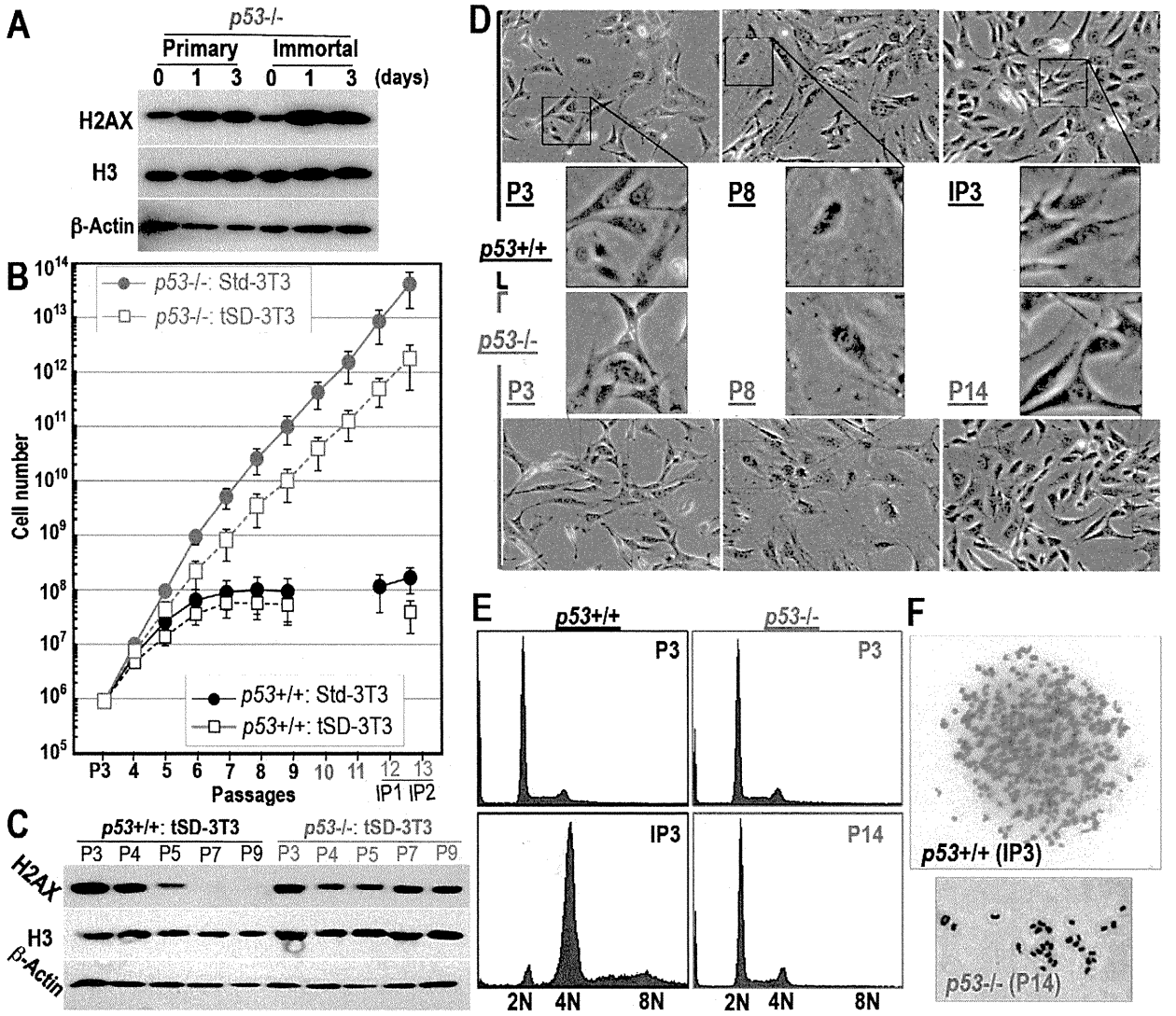

Figure 4. H2AX-diminished quiescent cell status is regulated by p53. A. DNA replication stress-associated H2AX diminution status was determined in *p53*-KO MEFs as in Figure 2E, in which H2AX was not down-regulated, even in primary MEFs. **B–F.** Primary *p53*-KO MEFs were cultured during the senescing and immortalizing processes (**B**). H2AX status was determined by Western blotting (**C**), morphological assessment (**D**), genomic status determined by flow-cytometry (**E**), and chromosome spread (**F**). Although *p53*-KO MEFs never showed major changes in H2AX expression, tetraploidization or growth arrest, *p53*-KO MEFs still exhibited a senescent morphology (P8) before achieving an immortalized morphology (P14).
doi:10.1371/journal.pone.0023432.g004

Mutation of the Arf/p53 module is induced with tetraploidization, triggered by DNA replication stress under moderately decreased H2AX levels in normal cells

Whereas *p53*-KO-MEFs are immortalized with diploidy (Fig. 4E, F), WT-MEFs are never immortalized only after tetraploidization [10] (Fig. 1B, C; Fig. 3B, C; Fig. 4E, F) and loss of Arf/p53 [22]. This suggests that the mutation of the Arf/p53 module in WT-MEFs is induced during tetraploidization. Supporting this argument, p53-dependent quiescence produced by diminished H2AX is maintained under diploidy preservation but abrogated after tetraploidization with mutation in the Arf/p53 module and the resulting H2AX recovery (Fig. 3). Therefore, normal WT-MEFs are protected from immortalization by a quiescent cell status, as long as the genome is preserved in diploidy. However, under continuous growth stimulation, tetraploidization also spontaneously arises in WT-MEFs but, unexpectedly, not in *p53*-KO-MEFs.

As tetraploidization was observed at the senescent stage under conditions of continuous growth stimulation that induce DNA replication stress (Fig. 3), the underlying reason for tetraploidization in WT-MEFs but not in *p53*-KO-MEFs might be associated with the repair deficiency that also occurs in an H2AX-diminished background. To examine the tetraploidization risk under an H2AX-diminished background, MEFs of each type were treated with HU for 36 hours and the incidence of bi-nucleated tetraploidy formation was compared (Fig. 5A). As expected, HU treatment-associated H2AX diminution (Fig. 2E) resulted in tetraploidization in primary WT-MEFs but not in immortalized WT-MEFs or p53-KO-MEFs (Fig. 5A). Thus, although normal cells become quiescent with largely diminished H2AX under diploidy, senescing cells with residual H2AX under growth stimulating conditions are potentially at risk of developing tetraploidy in response to DNA replication stress.

Finally, to address changes in DNA replication stress-sensitivity during serial proliferation of normal MEFs, the repair efficiencies

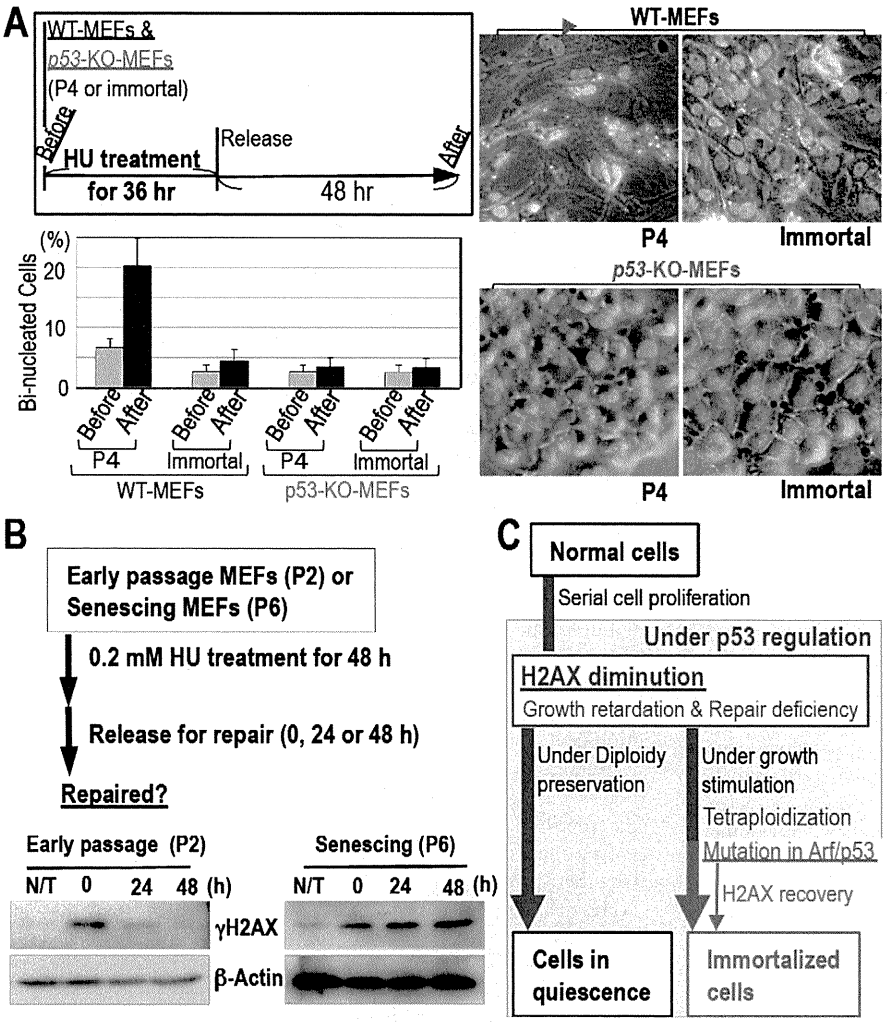

Figure 5. Increased risk of tetraploidization in normal MEFs. A. DNA replication stress-associated tetraploidization was determined in MEFs (P4) with the formation of bi-nucleated tetraploidy (red arrowhead) after 0.2 mM HU treatment as illustrated (top-left panel). Tetraploidization was efficiently induced during primary growth but not in immortalized MEFs or *p53*-KO-MEFs. **B.** Repair efficiencies of DNA replication stress-associated lesions were compared between early passage (P2) and senescing MEFs (P6) after 48 h hydroxyurea (HU) treatment. γH2AX signal was used as a marker of DNA lesions, in which γH2AX signal and β-Actin signals in senescing MEFs (P6) were detected only with over-exposure compared to early passage MEFs (P2), due to decreased H2AX levels during senescence. The reduction in γH2AX signal after release was only evident in early passage MEFs, which suggests that senescing cells are defective in resolving DNA replication stress. **C.** A model of MEFs under serial cell proliferation either undergoing quiescence or developing immortality. While MEFs that maintain quiescence and diploidy show diminished H2AX levels, MEFs developing immortality accumulate γH2AX foci.
doi:10.1371/journal.pone.0023432.g005

of DNA replication stress-associated lesions were compared between early passage and senescent MEFs with the decay of the γH2AX signal after release from HU treatment (Fig. 5B). Unlike early passage MEFs (P2), senescing MEFs (P6) were deficient in repairing HU-associated DNA lesions (Fig. 5B), in which MEFs show slow cell-cycle progression and residual H2AX expression. This is in contrast to quiescent MEFs with largely diminished H2AX level that show neither detectable cell cycle progression nor DNA replication stress. Thus, normal cells under serial proliferation decrease H2AX expression; thereby, cells slow growth activity and become defective in DNA repair. In such cells, cellular homeostasis is preserved by quiescence under largely diminished H2AX level regulated by p53 as long as diploidy is preserved. However, these cells are simultaneously at increased risk of tetraploidization with p53 dysfunction under continuous growth acceleration, resulting in the development of immortality and recovery of H2AX activity and cell growth (Fig. 5C).

Discussion

The results of this study revealed the following novel concepts: (i) normal cells generally achieve quiescent status with diminished H2AX level both *in vitro* and *in vivo*, and this is regulated by p53; (ii) growth arrested normal cells with senescent morphology can be defined as either (a) those in a continuous quiescent status with largely diminished H2AX level or (b) those in a transient status with inducing genomic instability and the resulting onset of immortality, under which cells accumulate γH2AX foci; (iii) to protect cells from immortality, one of the critical roles of p53 is the induction of growth-arrest via the down-regulation of H2AX with cellular quiescence. Cells in H2AX diminution-associated quiescence are shown in the cause of mature and premature senescence, during which cells show senescent morphology (Fig. S1), probably because these cells are repair defective (Fig. 5B). However such repair deficiency is also associated with genomic instability

development under accelerated growth stimulation, resulting in immortality acquisition with Arf/p53 module mutation and H2AX recovery.

Since growth-arrested cellular status with senescent morphology is directly induced by H2AX-knockdown (Fig. 2F), H2AX down-regulation is involved in a cause of quiescent cellular status. On the other hand, residual H2AX-expression in senescent cells is an associated effect for tetraploidization and immortalization: residual H2AX in senescent cells are only observed under accelerated growth stimulation (Figs. 1 and 3), under which cells are subjected to DNA replication stress and exhibit γH2AX, resulting in tetraploidization. Thus, even though cells are morphologically senescent with no growth in total cell number, cellular statuses could be either cells developing genomic instability under continuous growth acceleration (Std-3T3) or continuously quiescent cells under occasional arrest (tSD-3T3).

Unlike highly accumulated p53 that induces apoptosis, the Arf/p53 module under normal conditions functions for longevity by suppressing tumors in mice and giving protection from immortalization in MEFs [22]. Here, our results illustrated that such cellular status is produced with H2AX diminution-associated quiescence by protecting from immortalization under normal p53 regulation but is abrogated by Arf/p53 module mutation that is induced with tetraploidization under continuous growth stimulation, resulting in recovery of H2AX and growth activity. Unlike cells undergoing apoptosis, cells preserving quiescence under normal conditions do not accumulate p53 protein [10], which is probably associated with p53 function expression for quiescent status preservation but not for apoptosis induction. Intriguingly, such p53-dependent H2AX diminution was only observed after cells reach growth arrest both *in vivo* and *in vitro* but not growing cells in early passages and in organs from young mice (Fig. 2). In accordance with this, the expression of p53 targets Sidt2 and Phlda3, which are likely associated with tumor suppression [32], were elevated after cells become H2AX diminution-associated quiescent (P7) compared to cells in early passage (P3) (Fig. S6). However, similar to p53 protein, the increase in p53 transcript is also limited (Fig. S6). Thus, p53 function is expressed for apoptosis with accumulated p53, otherwise for H2AX-diminution associated quiescent status preservation under normal regulation without accumulating p53.

Except for tumors associated with specific chromosomal translocation, development of most cancers as well as *in vitro* cellular transformation is associated with genomic instability of either CIN or MIN [2,3]. Importantly, tetraploidization, a major initial form of CIN under a mismatch repair proficient background is induced with oncogenic stress by accelerated S-phase entry [10], leading to immortality acquisition in MEFs with mutation in the Arf/p53 module. Here, our results showed that quiescence could be preserved with largely diminished H2AX and diploidy preservation under the regulation of p53. Although H2AX down-regulation is only observed under functional p53 regulation, it is still unclear how p53 down-regulates H2AX. Our results showed the reduction of total H2AX transcript during the senescing process (Fig. S4) and a damage-induced decrease of H2AX protein under functional p53 regulation (Fig. 2E; Fig. 4A, B). Although p53 role for H2AX down-regulation is unclear, the regulation might be indirect because (1) there is no p53-binding site on the *H2AX* promoter, (2) there is no signal of the *H2AX* gene with ChIP-on-CHIP analyses against p53 [33], (3) H2AX expression does not associate with the activation level of p53 as we observed no association between H2AX expression and p53 activation (Fig. S7).

Together, our results provide a rationale for the regulation of cellular homeostasis preservation. By prohibiting immortality development and preserving quiescent cell status, p53 induces an H2AX diminution-mediated quiescent status. However, this status is abrogated by continuous growth stimulation, which results in the induction of genomic instability with mutation of the Arf/p53 module, which leads into H2AX recovery, the restoration of growth activity, and immortality acquisition (Fig. 5C).

Methods

Ethics Statement

Mice were treated in accordance with the Japanese Laws and the Guidelines for Animal Experimentation of National Cancer Center. All experiments were approved by The Committee for Ethics in Animal Experimentation of National Cancer Center (approval ID numbers: A59-09 and T07-038).

Cell culture and tissue samples

Cells were cultured as described previously [34]. Both wild-type and *p53*-KO MEFs were prepared from day 13.5 embryos of wild type and $p53^{(+/-)}$ mice [35] as previously described [34] and cultured under the standard 3T3 (Std-3T3) passage protocol [36] or with the following modifications: tSD-3T3. Senescing MEFs (P6 or P8) were maintained under tSD-3T3 conditions for the experiments shown in Figures 2, 3, 4, 5. NHFs (normal human umbilical cord fibroblasts; HUC-F2, RIKEN BRL Cell Bank) were cultured under Std-3T3 conditions. Resveratrol treatment of NHFs was performed as for MEFs. For the H2AX shRNA study, the reported sequence oligonucleotide [37,38] was inserted into the pSuper.retro.puro vector (Oligoengine) and the shRNA virus was then prepared using 293T cells. The virus was infected into NHF cells and selected with puromycin. Mouse tissue samples were prepared from mice at the ages indicated (Sankyo Labo Service).

DNA damage and induction of replication stress

DSB damage was induced by neocarzinostatin (Pola Pharma, Tokyo, Japan) treatment. For induction of DNA replication stress, MEFs were treated with hydroxyurea (HU).

Antibodies, immunostaining and Western blotting

Antibodies against γH2AX (JBW301, Upstate Biotechnology) and H2AX (Bethyl) were used for immunostaining and Western blot analysis. Antibodies against β-actin (AC-74, Sigma), PCNA (Santa Cruz) and histone H3 (ab1791, Abcam) were used for Western blot analysis. Prior to immunostaining with primary and secondary antibodies, cells were fixed with 4% paraformaldehyde for 10 min and permeabilized with 0.1% Triton X-100/PBS for 10 min. Western blot analysis and confocal microscopy were performed as described previously [10].

Transcription level analyses with RT-PCR

Total RNA was extracted from MEFs with the RNeasy system (Sigma). RNA (0.8 μg) was reverse-transcribed using a cDNA Archive kit (Applied Biosystems) and subjected to PCR. The following PCR primers were used: H2axf, 5′-TTGCTTC-AGCTTGGTGCTTAG-3′; H2axr, AACTGGTATGAGGC-CAGCAAC; β-actinf, CATCCAGGCTGTGCTGTCCCTGTA-TGC; and β-actinr, GATCTTCATGGTGCTAGGAGCCA-GAGC; Trp53-F, CGGATAGTATTTCACCCTCAAGATC-CG; Trp53-R, AGCCCTGCTGTCTCCAGACTC; Sidt2-F, CGGAAGGCTGGTTTCTGAGTTTCCG; Sidt2-R, CTGTA-AACGCCAAGGACCAGAA; Phlda3-F, CGGTCCATCTAC-

TTCACGCTAGTGACCG; Phlda3-R, TGGATGGCCTGTTGATTCTTGA; Gapdh-F, AACTTTGGCATTGTGGAAGG; Gapdh-R, ATGCAGGGATGATGTTCTGG. The amplified products by Ampli*Taq* Gold (Applied Biosystems) were separated on a 2% agarose gel and visualized with ethidium bromide. Otherwise, real-time PCR assay was carried out using Power SYBER green PCR Master kit (ABI).

Chromosome spreads

Mitotic cells were prepared by treatment with 20 ng/ml nocodazole for 6 h and then collected. The collected cells were swollen hypotonically with 75 mM KCl for 15 min, and then fixed with Carnoy's solution (75% methanol/25% acetic acid) for 20 min. After changing the fixative once, the cells were dropped in Carnoy's solution onto glass slides and air-dried. The slides were stained with 4% Giemsa (Merck) solution for 10 min, washed briefly in tap water, and air-dried.

Supporting Information

Figure S1 Representative images of MEFs during the lifespan. MEFs cultivated as in Figure 1A top lead into either immortality development under Std-3T3 or quiescence preservation under tSD-3T3. After serial cultivation, MEFs become morphologically senescent, i.e., flattened and enlarged morphology (P9) under both Std-3T3 and tSD-3T3 conditions. While continuous MEF-culture under tSD-3T3 preserved the quiescent status with continuously senescent morphology, continuous MEF-culture under Std-3T3 lead to the sporadic emergence of immortalized colony from the senescent MEFs. Immortalized MEFs (IP2) are morphologically escaped from senescence and rather similar to that in early passage (P3).
(TIF)

Figure S2 H2AX diminution is also observed in adult mice organs. Samples were prepared from five week (5W), five month (5M) and seven- or nine-month-old mice (7M or 9M). Compared to five months old organs, H2AX protein level is diminished in Testis (9M), Brain (7M), and Colon (7M), in which the diminution levels are lower than those in Liver, Spleen, and Pancreas. In Heart and Thymus, H2AX levels did not altered the alteration in through 5 weeks old to 7 or 9 months old.
(TIF)

Figure S3 H2AX diminution is also shown in damage induced premature senescence. Premature senescence was induced with NCS treatment as shown schematically in the top, in which each red arrowhead represents 100 ng/μl NCS treatment. Premature senescence by damage was induced with H2AX diminution, in which cells showed typical senescent morphology of flattened and enlarged.
(TIF)

Figure S4 H2AX transcript is decreased in quiescent MEFs. Decrease in H2AX mRNA level in senescing MEFs was observed by RT-PCR (right panel) and is compared with protein diminution (left panel).
(TIF)

Figure S5 H2AX over-expression accelerates immortality development in MEFs with tetraploidy. A. Experimental scheme of H2AX over expression. After transfection of H2AX-over expressing (H2AX-OE) or empty control vectors into early passage MEFs (P3), the transformed MEFs were selected, re-plated, and maintained in complete medium until immortalized cells appeared. **B.** Growth curves of MEFs during the experiments in A. MEFs before transfection and re-plating, MEFs transfected with H2AX-over-expressing vector, and MEFs transfected with empty control vector are indicated by black closed squares, red open circles, and black open diamonds, respectively. MEFs over-expressing H2AX showed accelerated development of immortality. **C.** H2AX status was determined as indicated in the figure. Although senescence was induced in the transfected and selected MEFs, H2AX over-expressing MEFs show higher levels of H2AX after the selection resulting in the development of immortality with H2AX recovery. **D.** Representative MEF images during accelerated immortality development with H2AX over-expression and controls. MEFs transfected with the H2AX over-expressing vector showed an efficient escape from senescence, while MEFs carrying the negative control vectors remained senescent with a flattened and enlarged morphology. **E,F.** Genomic instability status in immortalized MEFs (IP3) that were developed with H2AX over-expression was assessed by flow-cytometry (**E**) and Giemsa staining of M-phase chromosome (**F**).
(TIF)

Figure S6 p53 expression in senescing MEFs. To determine p53 expression in the cause of senescence, the expression levels of p53 and the targets (Sidt2 and Phlda3) that are likely associated with tumor suppression were compared between early passage (P2) and senescent MEFs (P7) under tSD-3T3 conditions. Along with H2AX diminution under p53 proficient background after serial cultivation, the expressions of Sidt2 and Phlda3 were observed in senescent MEFs (P7), in which the change in the expressed p53 transcript is limited.
(TIF)

Figure S7 p53 activation shown by miR34a expression in primary wt-MEFs after damage is not directly associated with H2AX expression levels at least for transcript regulation. A. To confirm p53 dependent DNA damage response, wt- and $p53^{-/-}$-MEFs in primary and immortal were treated with 200 ng/ml neocarzinostatin (NCS) for 6 hours and the expression of p53-target miR34a was assessed. As expected, miR34a expression was shown after NCS treatment in primary wt-MEFs (wild type) but neither in immortalized wt-MEFs nor in $p53^{-/-}$-MEFs. **B.** To determine the p53-activation associated change in the expression levels of H2AX transcript, mRNA levels of H2AX in MEFs treated as in **A** were analyzed. Whereas p53 is activated after NCS treatment in primary wt-MEFs, H2AX transcript levels were stable, suggesting no direct regulation by p53 transcription factor for H2AX expression. The PCR primers for miR34a were used from miRNA-specific primers (ABI) with snoRNA202 (ABI) for the control. Real-time PCR assay was carried out TaqMan microRNA assay kit (ABI).
(TIF)

Acknowledgments

We thank RIKEN BRL Cell Bank for the normal human umbilical cord fibroblast (NHF) cells (HUC-F2). We also thank K. Shimizu-Saito, M. Yanokura, and I. Kobayashi for technical support. We are grateful to S. Takeda, W. Bonner, P. Hsieh, K. Okamoto, and S. Nakada for critical reading of the manuscript and to T. Tsuzuki and Y. Nakatsu for critical discussion of the study.

Author Contributions

Conceived and designed the experiments: KY. Performed the experiments: YA H. Fuji H. Fukuda AI KS YY MS YI JU KY. Analyzed the data: H. Fuji KY. Contributed reagents/materials/analysis tools: SM NT YH HN MM. Wrote the paper: KY H. Fukuda HT.

References

1. Negrini S, Gorgoulis VG, Halazonetis TD (2010) Genomic instability–an evolving hallmark of cancer. Nat Rev Mol Cell Biol 11: 220–228.
2. Lengauer C, Kinzler KW, Vogelstein B (1997) Genetic instabilities in colorectal cancers. Nature 386: 632–627.
3. Lengauer C, Kinzler KW, Vogelstein B (1998) Genetic instabilities in human cancers. Nature 396: 643–649.
4. Stephans PJ, Greenman CD, Fu B, Yang F, Bignell GR, et al. (2011) Massive genomic rearrangement acquired in a single catastrophic event during cancer development. Cell 144: 27–40.
5. Vitale I, Galluzzi L, Senovilla L, Criollo A, Jemaà M, et al. Illicit survival of cancer cells during polyploidization and depolyploidization. Cell death differ, doi: 10.1038/cdd.2010.145.
6. Danes BS (1978) Increased in vitro tetraploidy: tissue specific within the heritable colorectal cancer syndromes with polyposis coli. Cancer 41: 2330–2334.
7. Dutrillaux B, Gerbault-Seureau M, Remvikos Y, Zafrani B, Prieur M (1991) Breast cancer genetic evolution: I. Data from cytogenetics and DNA content. Breast Cancer Res Treat 19: 245–255.
8. Heselmeyer K, Schröck E, du Manoir S, Blegen H, Shah K, et al. (1996) Gain of chromosome 3q defines the transition from severe dysplasia to invasive carcinoma of the uterine cervix. Proc Natl Acad Sci USA 93: 479–484.
9. Maley CC, Galipeau PC, Li X, Sanchez CA, Paulson TG, et al. (2004) The combination of genetic instability and clonal expansion predicts progression to esophageal adenocarcinoma. Cancer Res 64: 7629–7633.
10. Ichijima Y, Yoshioka K, Yoshioka Y, Shinohe K, Fujimori H, et al. (2010) DNA lesions induced by replication stress trigger mitotic aberration and tetraploidy development. PLoS One 5: e8821.
11. Bartkova J, Horejsí Z, Koed K, Krämer A, Tort F, et al. (2005) DNA damage response as a candidate anti-cancer barrier in early human tumorigenesis. Nature 434: 864–870.
12. Gorgoulis VG, Vassiliou LV, Karakaidos P, Zacharatos P, Kotsinas A, et al. (2005) Activation of the DNA damage checkpoint and genomic instability in human precancerous lesions. Nature 434: 907–913.
13. Sedelnikova OA, Horikawa I, Zimonjic DB, Popescu NC, Bonner WM, et al. (2004) Senescing human cells and ageing mice accumulate DNA lesions with unrepairable double-strand breaks. Nature Cell Biol 6: 168–170.
14. Nakamura AJ, Chiang YJ, Hathcock KS, Horikawa I, Sedelnikova OA, et al. (2008) Both telomeric and non-telomeric DNA damage are determinants of mammalian cellular senescence. Epigenetics Chromatin 1: 6.
15. Geigl JB, Langer S, Barwisch S, Pfleghaar K, Lederer G, et al. (2004) Analysis of gene expression patterns and chromosomal changes associated with aging. Cancer Res 64: 8550–8557.
16. Sherr CJ, Weber JD (2000) The ARF/p53 pathway. Curr Opin Genet Dev 10: 94–99.
17. Sherr CJ (1998) Tumor surveillance via the ARF-p53 pathway. Genes Dev 12: 2984–2991.
18. Matheu A, Maraver A, Serrano M (2008) The Arf/p53 pathway in cancer and aging. Cancer Res 68: 6031–6034.
19. Tyner SD, Venkatachalam S, Choi J, Jones S, Ghebranious N, et al. (2002) p53 mutant mice that display early ageing-associated phenotypes. Nature 415: 45–53.
20. Maier B, Gluba W, Bernier B, Turner T, Mohammad K, et al. (2004) Modulation of mammalian life span by the short isoform of p53. Genes Dev 18: 306–319.
21. Varela I, Cadiñanos J, Pendás AM, Gutiérrez-Fernández A, Folgueras AR, et al. (2005) Accelerated ageing in mic deficient in Zmpste24 protease is linked to p53 signalling activation. Nature 437: 564–568.
22. Matheu A, Maraver A, Klatt P, Flores I, Garcia-Cao I, et al. (2007) Delayed ageing through damage protection by the Arf/p53 pathway. Nature 448: 375–379.
23. Parrincello S, Samper E, Krtolica A, Goldstein J, Melov S, et al. (2003) Oxygen sensitivity severely limits the replicative lifespan of murine fibroblasts. Nature Cell Biol 5: 741–746.
24. Bassing CH, Chua KF, Sekiguchi J, Suh H, Whitlow SR, et al. (2002) Increased ionizing radiation sensitivity and genomic instability in the absence of histone H2AX. Proc Natl Acad Sci USA 99: 8173–8178.
25. Celeste A, Petersen S, Romanienko PJ, Fernandez-Capetillo O, Chen HT, et al. (2002) Genomic instability in mice lacking histone H2AX. Science 296: 922–927.
26. Bronson R, Lee C, Alt WF (2003) Histone H2AX: A dosage-dependent suppressor of oncogenic translocations and tumors. Cell 114: 359–370.
27. Bassing CH, Alt FW (2004) H2AX May Function as an Anchor to Hold Broken Chromosomal DNA Ends in Close Proximity. Cell Cycle 3: 149–153.
28. Bonner WM, Redon CE, Dickey JS, Nakamura AJ, Sedelnikova OA, et al. (2008) GammaH2AX and cancer. Nature Rev Cancer 8: 957–967.
29. Tsukuda T, Fleming AB, Nickoloff JA, Osley MA (2005) Chromatin remodelling at a DNA double-strand break site in Saccharomyces cerevisiae. Nature 438: 379–383.
30. Keogh MC, Mennella TA, Sawa C, Berthelet S, Krogan NJ, et al. (2006) The Saccharomyces cerevisiae histone H2A variant Htz1 is acetylated by NuA4. Genes Dev 20: 660–665.
31. Ikura T, Tashiro S, Kakino A, Shima H, Jacob N, et al. (2007) DNA damage-dependent acetylation and ubiquitination of H2AX enhances chromatin dynamics. Mol Cell Biol 27: 7028–7040.
32. Brady CA, Jiang D, Mello SS, Johnson TM, Jarvis LA, et al. (2011) Distinct p53 transcriptional programs dictate acute DNA-damage responses and tumor suppression. Cell 145: 571–583.
33. Ceribelli M, Alcalay M, Viganò MA, Mantovani R (2006) Repression of new p53 targets revealed by ChIP on chip experiments. Cell Cycle 5: 1102–1110.
34. Yoshioka K, Yoshioka Y, Hsieh P (2006) ATR kinase activation mediated by MutSα and MutLα in response to cytotoxic O6-methylguanine adducts. Mol Cell 22: 501–510.
35. Tatemichi M, Tazawa H, Masuda M, Saleem M, Wada S, et al. (2004) Suppression of thymic lymphomas and increased nonthymic lymphomagenesis in Trp53-deficient mice lacking inducible nitric oxide synthase gene. Int J Cancer 111: 819–828.
36. Todaro GJ, Green H (1963) Quantitative studies of the growth of mouse embryo cells in culture and their development into established lines. J Cell Biol 17: 299–313.
37. Lukas C, Melander F, Stucki M, Falck J, Bekker-Jensen S, et al. (2004) Mdc1 couples DNA double-strand break recognition by Nbs1 with its H2AX-dependent chromatin retention. EMBO J 23: 2674–2683.
38. Dimitrova N, de Lange T (2006) MDC1 accelerates nonhomologous end-joining of dysfunctional telomeres. Genes Dev 20: 3238–3243.

Augmented cell death with Bloom syndrome helicase deficiency

HIDEO KANEKO[1,2], TOSHIYUKI FUKAO[1], KIMIKO KASAHARA[1], TAKETO YAMADA[3] and NAOMI KONDO[1]

[1]Department of Pediatrics, Graduate School of Medicine, Gifu University, Gifu 501-1194; [2]Department of Clinical Research, Nagara Medical Center, Gifu 502-8558; [3]Department of Pathology, School of Medicine, Keio University, Tokyo 160-8582, Japan

Received December 20, 2010; Accepted March 28, 2011

DOI: 10.3892/mmr.2011.484

Abstract. Bloom syndrome (BS) is a rare autosomal genetic disorder characterized by lupus-like erythematous telangiectasias of the face, sun sensitivity, infertility, stunted growth, upper respiratory infection, and gastrointestinal infections commonly associated with decreased immunoglobulin levels. The syndrome is associated with immunodeficiency of a generalized type, ranging from mild and essentially asymptomatic to severe. Chromosomal abnormalities are hallmarks of the disorder, and high frequencies of sister chromatid exchanges and quadriradial configurations in lymphocytes and fibroblasts are diagnostic features. BS is caused by mutations in BLM, a member of the RecQ helicase family. We determined whether BLM deficiency has any effects on cell growth and death in BLM-deficient cells and mice. BLM-deficient EB-virus-transformed cell lines from BS patients and embryonic fibroblasts from $BLM^{-/-}$ mice showed slower growth than wild-type cells. BLM-deficient cells showed abnormal p53 protein expression after irradiation. In $BLM^{-/-}$ mice, small body size, reduced number of fetal liver cells and increased cell death were observed. BLM deficiency causes the up-regulation of p53, double-strand break and apoptosis, which are likely observed in irradiated control cells. Slow cell growth and increased cell death may be one of the causes of the small body size associated with BS patients.

Introduction

Bloom syndrome (BS) is a rare genetic disorder caused by mutations in BLM, a member of the RecQ helicase family (1). There are five human RecQ-like proteins (RECQL1, BLM, WRN, RECQL4 and RECQ5), each having 3' to 5' DNA helicase activity, but little sequence similarity outside the helicase motifs (2,3). Three of these helicases (BLM, WRN and Rothmund-Thomson) show genomic instability and cancer susceptibility; however, each also has distinctive features (4,5). The unique features of BS are severe pre- and post-natal growth retardation and a wide spectrum of cancer types that develop at a young age. Other BS phenotypes include facial sun sensitivity, immunodeficiency and male sterility/female subfertility (6,7). Compared with Werner syndrome, small body size is one of the characteristic features associated with BS patients.

Here, we determined whether BLM deficiency has any effects on the cell growth and death of BLM-deficient cells and mice.

Materials and methods

BS patient. AsOk, who was identified in the BS registry as number 97, weighed 2,250 g at birth. Café-au-lait spots and mandibular hypoplasia were prominent. A 3-bp deletion was detected in the BLM sequence of AsOk DNA (8). This deletion caused the generation of a stop codon at amino acid 186.

Cell culture. EB-virus-transformed cell lines from BS patients and control subjects were developed as previously reported (9). In brief, PBMCs were isolated from the heparinized blood of patients by gradient centrifugation in Ficoll-Paque (Pharmacia AB, Uppsala, Sweden), and suspended at a density of 10^6 ml in culture medium consisting of RPMI 1640 supplemented with 10% heat-inactivated fetal calf serum, l-glutamine (2 mmol/l), penicillin (100 U/ml) and streptomycin (100 μg/ml). The PBMCs (10^6 ml) were then cultured in the presence of 10 μg/ml phytohemagglutinin (PHA) for 3 days.

Detection of p53 protein. PBMCs cultured with PHA for 3 days were irradiated (6 Gy). After 1 h, the cells were collected by centrifugation and protein was extracted. Using anti-human p53 antibody (Santacruz, USA), immunoblotting was performed.

BLM-deficient embryonic fibroblasts. Heterozygous BLM-deficient ($BLM^{+/-}$) mice were kindly provided by P. Leder. $BLM^{-/-}$ mice were obtained by mating $BLM^{+/-}$ mice (10). Embryonic fibroblasts from $BLM^{-/-}$ mice were obtained from 12.5-day embryos. None of the $BLM^{-/-}$ embryos survived more than 13 days.

Cell proliferation assay. Cell proliferation and cell viability were determined by the trypan blue or MTT assays. The MTT assay was performed following the manufacturer's protocol.

Correspondence to: Professor Hideo Kaneko, Department of Pediatrics, Graduate School of Medicine, Gifu University, 1-1 Yanagido, Gifu 501-1194, Japan
E-mail: hideo@gifu-u.ac.jp

Key words: Bloom syndrome, small body size, BLM deficiency, cell death

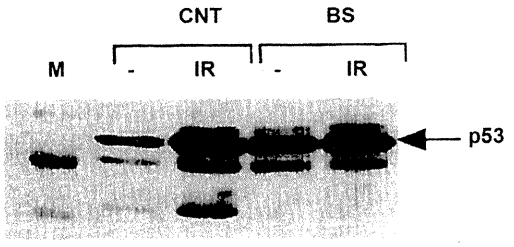

Figure 1. p53 protein expression in PBMCs from a control subject and a BS patient. PBMCs cultured with PHA for 3 days were irradiated (6 Gy). After 1 h, the cells were collected and p53 protein expression was detected.

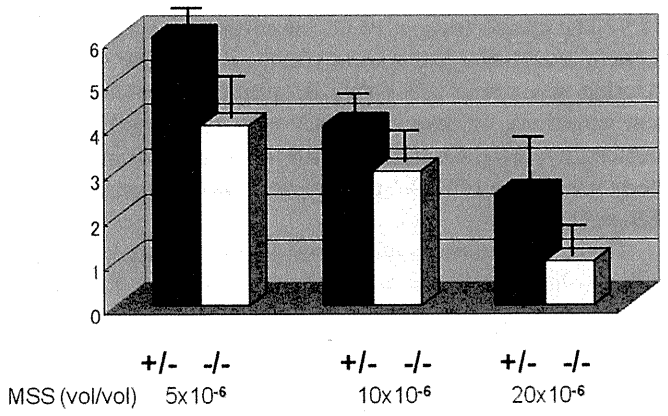

Figure 2. Fig. 2 Cell proliferation and cell viability were determined using trypan blue. Embryonic fibroblasts were established from $BLM^{+/-}$ and $BLM^{-/-}$ mice at 12.5 days post-coitus. Embryonic fibroblasts from $BLM^{-/-}$ mice showed a slow growth rate and a high sensitivity to MMS compared to those from $BLM^{+/-}$ mice.

Embryonic fibroblasts were cultured with methyl methanesulfonate (MMS) (Sigma, Japan) for 24 h (11), then the viable cell number was determined on trypan blue.

Detection of single-strand DNA. Paraffin and cryostat sections were prepared from the brain of $BLM^{+/-}$ or $BLM^{-/-}$ mice at 12.5 days post-coitus. Polyclonal rabbit anti-ssDNA antibody (IgG, 100 μg/ml, Dako Japan, Kyoto, Japan) at a dilution of 1:300 was used to detect the formation of single-stranded DNA (ssDNA) for 1 h at room temperature. Immunoreactivity was detected with peroxidase-labeled goat anti-rabbit immunoglobulins.

Results

Abnormal regulation of p53 protein expression. After the irradiation of PHA-stimulated PBMCs, p53 protein expression was induced in control cells (Fig. 1). In the PBMCs of the BS patient, high p53 protein expression was detected even without irradiation. Irradiation slightly induced p53 protein in BS cells. In the BS EB cell line, p53 phosphorylation by ATM was up-regulated compared with that in the control EB cell line (data not shown). These results suggested that BLM-deficient cells have abnormal regulation of p53 protein expression and an elevated frequency of apoptosis. Next, apoptosis was investigated *in vivo* and *in vitro* using BLM-deficient cells.

Slow growth in BLM-deficient cells. The growth rate of EB cells from BS patients was slower than that of control cells. After irradiation, the growth rate of BS cells was slower than that of control cells. MMS action caused double-stranded DNA breaks. The sensitivity of $BLM^{-/-}$ cells to MMS was higher than that of wild type cells. Embryonic fibroblasts originating from $BLM^{-/-}$ mice also showed a slowed growth rate (Fig. 2).

Augmented cell death in embryonic brain of $BLM^{-/-}$ mice. Anti-single-stranded DNA was detected in the brain of $BLM^{-/-}$ mice, with the number being higher than that detected in the brain of $BLM^{+/-}$ mice (Fig. 3). This result suggested the occurence of augmented cell death in $BLM^{-/-}$ mice.

Discussion

In this study, we showed the abnormal regulation of p53 protein expression and augmented cell death in BLM-deficient cells both *in vitro* and *in vivo*. Stalled replication forks can result in double-strand breaks, thereby triggering the activation of ATM (12). Consistent with a previously reported study, the deficiency of BLM was radiomimetic (13).

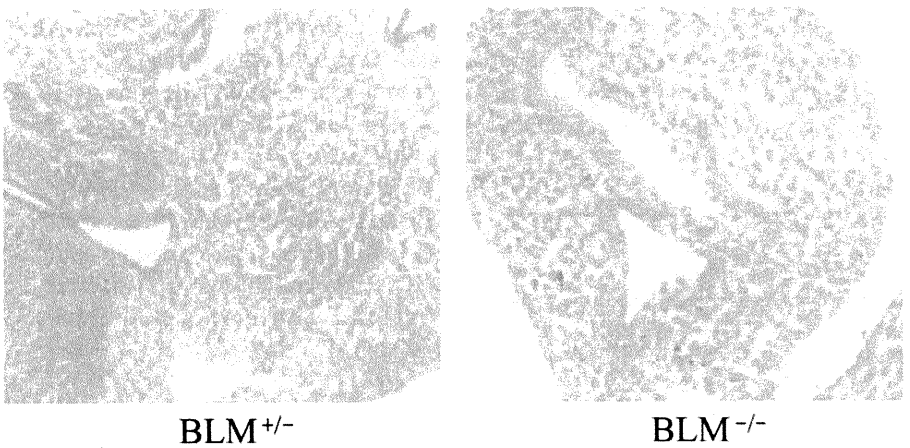

Figure 3. Detection of single-stranded DNA. Immunohistochemical staining of $BLM^{+/-}$ and $BLM^{-/-}$ embryos at 12.5 days post-coitus was performed.

Originally, MMS was considered to directly cause double-stranded DNA breaks, since homologous-recombination-deficient cells are particularly vulnerable to the effects of MMS. However, it is now considered that MMS stalls replication forks, and cells that are homologous-recombination-deficient have difficulty repairing the damaged replication forks.

Studies in yeast and human cells suggest a pivotal role of RECQ-like helicases in maintaining genomic integrity during the S phase (14). BS patients show small body size from birth. This small body size persists throughout their lifetime. At 12.5 days post-coitus, BLM-deficient mice have a smaller body size than wild-type mice (10).

BLM deficiency renders cells highly susceptible to apoptosis, which is a possible explanation for the pre- and post-natal growth retardation observed in BS patients. In the absence of BLM, many cells fail to repair damage rapidly enough, whereupon p53 signals those cells to die. Individuals with BS may continually lose cells, owing to excessive apoptosis, particularly during pre- and post-natal development, when cell proliferation is excessive (15). Excessive apoptosis would leave many tissues with chronic cellular insufficiency, and hence a small size, thereby explaining the pre- and post-natal growth retardation.

p53 is crucial for the apoptosis of BS cells. This apoptosis is not accompanied by an increase in BAX or p21 protein expression. Thus, p53 may induce apoptosis independent of its transactivation activity, consistent with the finding that p53 is transcriptionally inactive during the S phase. p53 may mediate the death of damaged BS cells by directly inducing mitochondria-mediated apoptosis, or by means of its transactivation activity.

In conclusion, BLM deficiency causes the dysregulation of p53 and augmented apoptosis, similar to that observed in irradiated wild-type cells. This slow cell growth and increased cell death may cause the small body size associated with BS patients.

Acknowledgements

This study was supported in part by Health and Labor Science Research Grants for Research on Intractable Diseases from The Ministry of Health, Labor and Welfare of Japan.

References

1. Ellis NA, Groden J, Ye TZ, *et al*: The Bloom's syndrome gene product is homologous to RecQ helicases. Cell 83: 655-666, 1995.
2. Ellis NA, Sander M, Harris CC and Bohr VA: Bloom's syndrome workshop focuses on the functional specificities of RecQ helicases. Mech Ageing Dev 129: 681-91, 2008.
3. Rossi ML, Ghosh AK and Bohr VA: Roles of Werner syndrome protein in protection of genome integrity. DNA Repair: Jan 13, 2010 (E-pub ahead of print).
4. German J: Bloom syndrome: a Mendelian prototype of somatic mutational disease. Medicine 72: 393-406, 1993.
5. Kaneko H and Kondo N: Clinical features of Bloom syndrome and function of the causative gene, BLM helicase. Expert Rev Mol Diagn 4: 393-401, 2004.
6. German J: Bloom's syndrome. Dematol Cli 13: 7-18, 1995.
7. German J and Ellis NA: Bloom syndrome. In: The Genetic Basis of Human Cancer. 1st edition. Vogelstein B and Kinzler (eds) McGraw Hill, New York, NY, pp301-315, 1998.
8. Kaneko H, Isogai K, Fukao T, *et al*: Relatively common mutations of the Bloom syndrome gene in the Japanese population. Int J Mol Med 14: 439-42, 2004.
9. Kaneko H, Matsui E, Fukao T, Kasahara K, Morimoto W and Kondo N: Expression of BLM gene in human hematopoietic cells. Clin Exp Immunol 118: 285-289, 1999.
10. Chester N, Kuo F, Kozak C, O'Hara CD and Leder P: Stage-specific apoptosis, developmental delay, and embryonic lethality in mice homozygous for a targeted disruption in the murine Bloom's syndrome gene. Genes Dev 12: 3382-3393, 1998.
11. Lundin C, North M, Erixon K, Walters K, Jenssen D, Goldman ASH and Helleday T: Methyl methanesulfonate (MMS) produces heat-labile DNA damage but no detectable in vivo DNA double-strand breaks. Nucleic Acids Res 33: 3799-3811, 2005.
12. Beamish H, Kedar P, Kaneko H, *et al*: Functional link between BLM defective in Bloom's syndrome and the ataxia-telangiectasia mutated protein, ATM. J Biol Chem 277: 30515-30523, 2002.
13. Horowitz DP, Topaloglu O, Zhang Y and Bunz F: Deficiency of Bloom syndrome helicase activity is radiomimetic. Cancer Biol Ther 7: 1783-1786, 2008.
14. Oh SD, Lao JP, Hwang PY, Taylor AF, Smith GR and Hunter N: BLM ortholog, Sgs1, prevents aberrant crossing-over by suppressing formation of multichromatid joint molecules. Cell 130: 259-272, 2007.
15. Dvalos AR and Campis J: Bloom syndrome cells undergo p53-dependent apoptosis and delayed assembly of BRCA1 and NSB1 repair complexes at stalled replication forks. J Cell Biol 29: 1197-1209, 2003.